Journal for Electrochemistry and Plating Technology

JEPT

Edited by: DGO-Fachausschuss Forschung – Hilden / Germany

ELECTROCHEMICAL NUCLEATION AND GROWTH OF GOLD ON EMBEDDED RHENIUM NANOWIRES

The formation of gold nanoelectrode arrays was investigated by electrodeposition of the metal along the pores left on directionally solidified NiAl-Re eutectics by selective dissolution of the rhenium fibre. After the necessary pre-treatment for the passivation of the NiAl matrix and dissolution of the rhenium fibres to create arrays of nanopores (diameter ~ 400 nm), the electrodeposition of gold into the pores was initially investigated by examining the growth of the deposits with the application of cathodic pulses. It was observed that the size of the gold deposits increased with the duration of the applied cathodic pulse once an initial charge of ~ 800 C/m^2 was overcome. The necessity of applying charges larger than that to observe significant deposits is due to the occurrence of a series of processes alongside the electrodeposition: charging of the oxides present on the eutectic and reduction of any remaining rhenium...

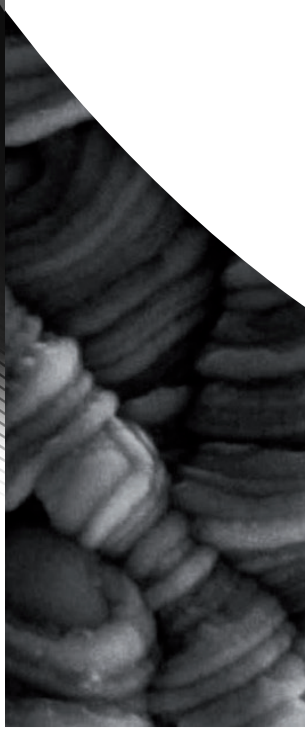

Received: 2007-12-16
Received in revised form: 2008-05-17
Accepted: 2008-07-10

Keywords: electrodeposition, nucleation, rhenium oxidation

By B. B. Rodriguez and A. W. Hassel

LEUZE VERLAG
seit 1902

Electrochemical Nucleation and Growth of Gold on Embedded Rhenium Nanowires

By Belen Bello Rodriguez and Achim Walter Hassel, Max-Planck-Institut für Eisenforschung GmbH, Düsseldorf, Germany

The formation of gold nanoelectrode arrays was investigated by electrodeposition of the metal along the pores left on directionally solidified NiAl-Re eutectics by selective dissolution of the rhenium fibre. After the necessary pre-treatment for the passivation of the NiAl matrix and dissolution of the rhenium fibres to create arrays of nanopores (diameter ~ 400 nm), the electrodeposition of gold into the pores was initially investigated by examining the growth of the deposits with the application of cathodic pulses. It was observed that the size of the gold deposits increased with the duration of the applied cathodic pulse once an initial charge of ~ 800 C/m^2 was overcome. The necessity of applying charges larger than that to observe significant deposits is due to the occurrence of a series of processes alongside the electrodeposition: charging of the oxides present on the eutectic and reduction of any remaining rhenium oxide on the rhenium fibres. Electrodeposition under potentiostatic conditions yielded a better control over the obtained gold structures, and enabled the selective filling of the pores. However, the recorded current transients under those experimental conditions did not obey any of the proposed models for nucleation and growth accurately. This was explained by the simultaneous formation of rhenium oxides and the interference of this process on the recorded current. Nevertheless, the studies reported give initial information on the electrochemical processes that take place when complex metallic substrates are employed for electrodeposition.

Keywords: electrodeposition, nucleation, rhenium oxidation

Paper*: Received:* 2007-12-16 / ***Received in revised form***: 2008-05-17 / ***Accepted***: 2008-07-10

1 Introduction

Electrodeposition is a very common technique for the production of materials with applications in diverse fields. In particular, electrodeposited metals have found applications as sensors, for contacting semiconductors, protective coatings (electrozinc, electronickel), or decorative finishing (jewellery), to name a few [1]. The properties and characteristics of the metallic electrodeposits must be tuned according to their application, and therefore the optimization of the electrodeposition process is of great significance. The electrodeposition of metals on foreign substrates has been extensively investigated in recent years. Some studies have focused on the morphologies obtained during the deposition [2], but most efforts have been dedicated to the determination of the nucleation and growth processes in order to understand the general electrodeposition process [3–7].

Serruya et al. studied the kinetics of the nucleation and diffusion-controlled growth of mercury species from the analysis of potentiostatic current transients [3]. They found that the distribution of the deposited nuclei was more uniform when the process took place at low overpotentials. This principle was described by *Schultze* et al. [4]. *Stoychev* et al. looked at the suitability of different substrates for the electrodeposition of platinum [5]. They examined the cyclic voltammograms recorded for the deposition of platinum on a wide range of electrodes, and from the obtained current transients they established the nucleation and growth processes in each example. They concluded that, of the investigated materials, tungsten, titanium and glassy carbon electrodes were suitable for nucleation and growth studies. The electrodeposition of gold on different n-GaAs crystal faces was investigated by *Depestel* and *Strubbe* [6] by use of chronoamperometric current transients and atomic force microscopy. The authors reported a difference in the nucleation mechanism depending on the surface orientation of the crystal, as well as on the deposition potential. The effect of the applied potential on

the nucleation mechanism was also determined for the deposition of a gold-nickel alloy [7]. The nucleation mechanism changed from progressive at low overpotentials to instantaneous at high overpotentials for the deposition of gold-nickel. The number of nucleation sites was also found to increase with the potential in this study.

There is a huge number of publications which have focused on the development of expressions and theories for the modelling of nucleation and growth mechanisms. It is out of the scope to review them in this work and therefore only three examples shall be cited here. *Heerman* and *Tarallo* propose a theory that enabled to describe the amperometric current transients obtained for the electrochemical nucleation and diffusion controlled growth on microelectrodes [8]. The diffusion controlled growth of hemispheres in ordered arrays was modelled by *Scharifker* [9]. In this case, the initial growth of deposits triggered an increase in the current, whereas the diffusion controlled growth dropped the current value significantly. A comprehensive set of studies has been performed on the aspects of nucleation by *Kolb* and his co-workers from which an atomistic view of the electrodeposition was derived [10].

The aim of the reported investigation is to study the kinetics of the nucleation and growth of gold hemispheres in the pores formed in directionally solidified NiAl-Re eutectics by selective dissolution of the rhenium fibrous phase. The use of these eutectics enables to produce arrays of nanoelectrodes regarding that the gold deposits grow exclusively along the nanopores. This can be achieved by discriminating the nucleation and growth mechanisms involved in the electrodeposition process, and therefore confining the experimental procedure to the time scale at which diffusion limited growth of the deposits does not dominate the process.

On one side the evolution of the gold deposits with time following the application of short cathodic pulses for the electrodeposition was studied. On the other side the current transients obtained for the process are evaluated in order to determine the formation and growth of nuclei, and the range at which each of these processes governs the electrodeposition. As a result, the best experimental conditions (deposition potential, concentration of electrolyte, duration of the process) for the formation of gold structures into the pores were obtained, avoiding their growth outside the pores. This way, the final surface can be described as an array of gold hemispheres deposited in the excavated nanopores, and uniformly distributed on the samples surface.

2 Materials and methods

NiAl-Re eutectics were directionally solidified as described previously [11]. As a starting material, nickel (99.97 wt.%), electrolytic aluminium (99.9999 wt.%) and rhenium pellets (99.9 wt.%) were used for the alloy preparation The directional solidification was conducted at a temperature of 1690 ± 10 °C, a thermal gradient of approximately 40 K/cm and a growth rate of 8.3 µm/s. Samples were cut normal to the solidification direction. A diameter of 400 nm was found for the rhenium wires, and the mean inter fibre spacing was 3 µm in agreement with the solidification kinetics determined for this system [12]. The fibre orientation was (100) referring to the rod axis of the directionally solidified sample.

The electrochemical passivation of the NiAl matrix prior to the electrodeposition of gold was carried out by polarization of the eutectic alloy at 0.7 V vs. SHE in 1 M acetate buffer (pH = 6.0). A conventional three-compartment cell (approx. volume 50 mL) with working, reference and counter electrodes was employed in all experiments. The samples were mechanically mirror-like ground prior to measurements. The counter electrode was a smooth gold foil with an apparent surface area of 2 cm^2 and a commercial Ag/AgCl electrode was used as reference (*Metrohm*, Filderstadt, Germany). A *PST050* potentiostat (*Radiometer Analytical*, Lyon, France) was used in all electrochemical measurements. Measurements were performed at room temperature in quiescent solutions. All potentials are given versus the standard hydrogen electrode (SHE).

The electrodeposition of gold was carried out from a commercial bath containing 12 g/L of gold sulphite (in the form of $(NH_4)_3[Au(SO_3)_2]$) in neutral pH buffer (*Metakem*, Usingen, Germany) for which compositional details were studied by *Osaka* et al. [13]. For the studies on the evolution of the deposits with the deposition time and potential, the plating

was carried out by application of rectangular reverse pulses [14]. The potential was switched from -0.7 V to 0.1 V (against anode) with a ratio of anodic duration to cathodic duration of 1:10 s. The duration of the cathodic pulse was varied from 1 ms to 3 s, and the concentration of gold(I) was kept constant at 76 mM. The studies on the nucleation and growth of the gold deposits were carried out by running potentiostatic measurements at -0.7 V vs. counter electrode and examining the recorded current transients. These experiments were performed with different concentrations of gold(I) (1.5 mM to 76 mM), after appropriate dilution of the plating bath in 0.1 M Na_2SO_4. All experiments were performed at room temperature in non deaerated solutions.

Cyclic voltammetric analyses of the ammonia gold sulfite plating bath were carried out in the three-compartment electrochemical cell, with a gold counter electrode (apparent area = 2 cm^2), a Ag/AgCl reference electrode (connected to the cell by a *Luggin capillary*), and a platinum microelectrode as working electrode (diameter = 15 µm). The platinum electrode was employed instead of a rhenium wire to avoid any interference in the measurements arising from the oxidation of the rhenium electrode. The scans were started at OCP (64 mV vs. Ag/AgCl), then progressed in a cathodic direction to -1 V, anodically to 1 V (vs. the employed Ag/AgCl reference electrode), and then back to OCP. The scan rate was 10 mV/s.

Scanning electron microscopy pictures were obtained on a *Leo 1550 VP* apparatus (*Leo Elektronenmikroskopie GmbH*, Oberkochen, Germany) fitted with an *INCA* Energy Dispersive System (*EDS*) (*Oxford Instruments*, Oxford, UK).

All materials used were of analytical grade and purchased from *Merck* (Darmstadt, Germany).

3 Results and discussion

3.1 Evolution of gold deposits with the duration of the electrodeposition process

The studies previously reported on the electrodeposition of gold using NiAl-Re alloys as substrates [15, 16] were taken as a starting point for the investigations reported here. In the mentioned work, the application of consecutive pulses resulted in the formation of gold microspheres whose behaviour resembled that of a conventional microelectrode. In order to improve the response of the formed gold electrodes, and to approach that of an array of nanoelectrodes, initial studies focused on the control over the deposition time for the selective deposition of the gold structures on the nanopores. Therefore, short cathodic pulses were applied (1 ms to 1 s), followed by 10-times longer anodic pulses to allow diffusion of the ions from the bulk solution, thus minimizing any halt in the reaction due to a depletion of gold(I) ions on the electrode/solution interface. In this set of experiments, the initial passivation of the NiAl matrix was performed at 0 V. At this potential, the rhenium fibers remain insoluble and the gold deposition takes place on their surface [16]. Deposition on the surface of the fibres, rather than at the bottom of the pores, enables a better optical characterization of the developing structures, since it overcomes the limitations of light transmission into deep narrow pores.

The evolution of the size of the gold deposits with the duration of the applied cathodic pulse is shown in *Figure 1*. For cathodic pulses of 10 ms, the gold deposits are only observed after the application of more than 100 consecutive cycles (1 s total deposition time); when the cathodic pulses have a duration of 50 ms, only 20 consecutive cycles are required to observe a significant amount of gold deposits (1 s total deposition time). For cathodic pulses with duration ≥ 100 ms, the deposition of gold takes place almost instantaneously, and well defined gold structures are observed even after the applica-

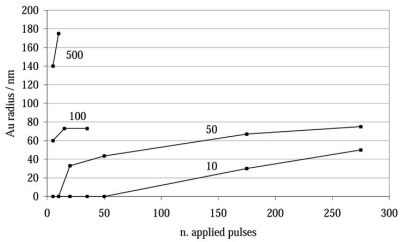

Fig. 1: Increase in the size of the obtained gold deposits with the number of applied cathodic pulses for pulses of increasing duration

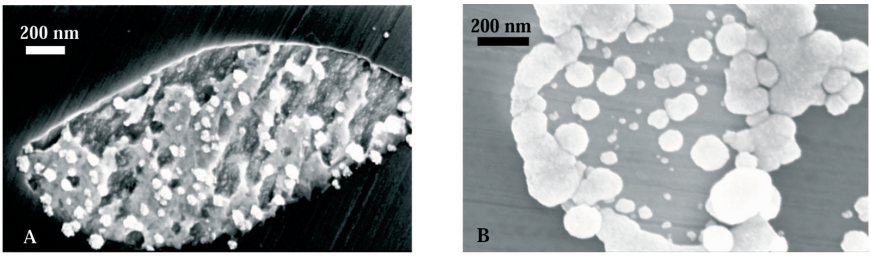

Fig. 2: Gold deposits obtained on NiAl-Re by application of cathodic pulses at -0.7 V (vs. counter electrode) followed by anodic pulses at 0.1 V (vs. counter electrode): A) 50 ms cathodic pulses applied for 4 s, and B) 500 ms cathodic pulses applied for 2.5 s

tion of very few cycles. The size of the deposits, determined by the average radius of the structures, also increased for cathodic pulses ≥ 100 ms. From these results, it can be concluded that the minimum deposition time required for the formation of gold deposits is ~ 1 s. The structures obtained in each case are shown in *Figure 2*.

The fact that a large number of cycles is needed when the duration of the cathodic pulse is < 100 ms indicates that not all the charge applied with each pulse is consumed in the creation of gold nuclei. Integration of the current density obtained for any individual cathodic pulse (1 ms to 3 s) gave the charge associated with each investigated pulse. From the charge, the theoretical mass of gold which would be deposited on the sample with each pulse (assuming 100 % efficiency of the process) was calculated according to *equation <1>:*

$$Q = {}^{(mzF)}/_{M}$$

or

$$q = {}^{(mzF)}/_{(MA)} \qquad <1>$$

where Q is the integrated charge, z the number of exchanged electrons, F the Faraday constant, and M the molar weight of the metal. If the charge Q is normalized to the electrode Area A, it is referred to as charge density q. Both, the charge density and the amount of gold deposited increased with the duration of the pulse (*Tab. 1*). From these calculations one could conclude that the deposition of gold takes place after the application of the first pulse in all cases. However, the experimental investigations described so far demonstrated that for very short cathodic pulses (< 100 ms), the application of at least 10 consecutive cycles was essential to produce significant nuclei. Considering a charge density of 8 C/m^2 (for a pulse of 10 ms), and a minimum of 100 pulses required to observe a significant amount of gold nuclei on the fibres, it can be concluded that, from the total charge of ~ 800 C/m^2 a significant amount is consumed in a process other than the electrodeposition. Recent studies on the anodic polarization of the ds-NiAl-Re samples in acetate buffer before the electrodeposition of gold revealed a series of reactions that occur simultaneously on the sample [16]: growth of aluminium oxide (Al_2O_3) and nickel oxide (NiO), oxidation of rhenium to form oxides of different natures, and their further conversion to soluble perrhenate species. Therefore, and during the electrodeposition process, it is expected that part of the applied charge is consumed in charging of the different oxides, double layer charging, and reducing films of rhenium oxides that may block the fibre surface.

The evolution of the formation of gold deposits on ds-NiAl-Re samples when the duration of the applied cathodic pulses was varied between 1 ms to 3 s was also investigated after the samples pretreatment at 0.7 V for the formation of nanopores [15]. In this case, the gold deposits are expected to grow along the nanopores, creating arrays of gold nanowires before protruding from the pores (*Fig. 3*). The charge density and mass of gold deposited (assuming 100 % efficiency) increased with the duration of the cathodic pulses, as observed in the previous experiments (*Tab. 1*). However, due to the large concentration of gold in the electrolyte, the

Tab. 1: Increase in the charge applied with each cathodic pulse with the duration of the pulse

	System					
	Rhenium fibres		*Rhenium pores*		*Rhenium wire*	
Pulse duration (s)	*Q (C/m²)*	*Au mass (µg/cm²)*	*Q (C/m²)*	*Au mass (µg/cm²)*	*Q (C/m²)*	*Au mass (µg/cm²)*
0.001	10.12	2.1	1.02	0.21	50.6	10.3
0.01	8.51	1.7	6.22	1.27	74	15.1
0.05	23.9	4.9	18.32	3.74		
0.1	147	30	70.2	14.3	78	16
0.5	117	24				
1	233	47	384	78.3	329	67
3			1423	290		

process was determined by the diffusion controlled growth of the gold deposits. As a result, the formation of gold nanoelectrodes was not achieved. A theoretical approximation of the deposition time required to achieve the filling of the pores is not feasible under these circumstances, since the experimental results obtained suggested the co-existence of other electrochemical processes.

3.2 Nucleation and growth of gold into rhenium nanopores

The experiments described in the previous section (*section 3.1*) enabled to determine the evolution of the gold deposits with the duration of the applied process, but the conditions employed in all tests were not optimal for the formation of gold nanoelectrodes by selective filling of the pores. Therefore, further optimization of the electrodeposition process was performed to ensure the growth of the gold deposits exclusively along the pores left by the dissolution of the rhenium fibres.

Variation of the deposition time, while keeping constant the 1:10 ratio between cathodic and anodic pulses and the concentration of the plating bath, resulted in the formation of gold hemispheres which showed an electrochemical behaviour comparable to that of a conventional microelectrode [15]. The formation of such large spheres results from the high concentration of the electrolyte, which allows continuous growth under diffusion control once the pores are filled. This assumption is corroborated by an analysis of the current transients recorded for the plating process. In order to move the growth of the gold deposits away from the diffusion region, and to separate the nucleation and growth processes,

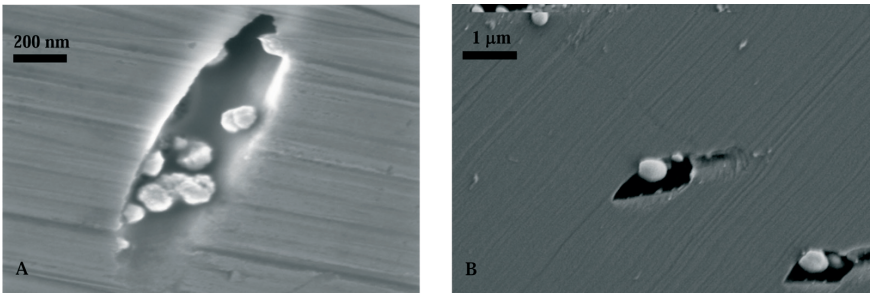

Fig. 3: Gold deposits obtained in rhenium pores by application of cathodic pulses at -0.7 V (vs. counter electrode) followed by anodic pulses at 0.1 V (vs. counter electrode): A) 100 ms cathodic pulses applied for 10 s, and B) 1 s cathodic pulses applied for 5 s

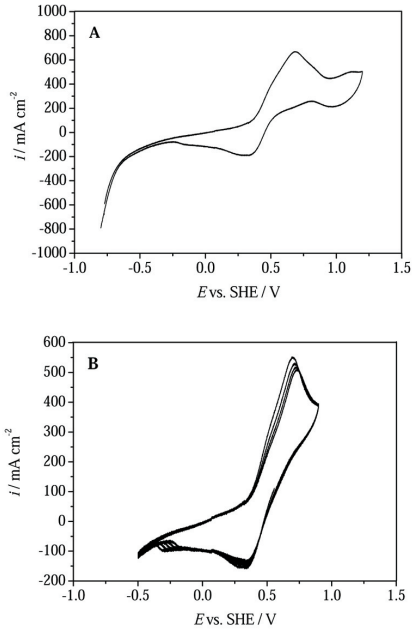

Fig. 4: Cyclic voltammograms obtained for 3.8 mM $(NH_4)_3[Au(SO_3)_2]$ (WE = Pt, RE = Ag/AgCl, CE = Au, 10 mV/s): A) potential swept from -0.8 V to 1.2 V (vs. SHE); B) potential swept from -0.5 V to 1 V (vs. SHE)

further experiments were run potentiostatically in very diluted electrolyte concentrations. A detailed examination of the current transients recorded will enable to separate the nucleation and growth mechanisms from the overall process.

The potential at which the deposition will be carried out was determined from the i / E plots recorded for the potentiodynamic polarization of a solution containing 3.8 mM $(NH_4)_3[Au(SO_3)_2]$. *Figure 4a* shows the current density recorded when the potential was swept between -0.8 V and 1.2 V vs. SHE. The reduction scan is characterized by a large current peak rising at -0.5 V, attributable to the reduction of gold(I) ions to gold(0). In the reverse anodic scan, a large oxidation peak is observed at 0.7 V, and a smaller one at 1.0 V. The intensity of the first peak did not decrease significantly after successive scans, as shown in *Figure 4b*. The following cathodic scan displayed two small reduction peaks at 0.9 V and 0.3 V, followed by a current loop that starts at 0.0 V and evolves into a peak at -0.2 V, just before the reduction of gold(I) becomes visible.

Gold deposition from a sulfite complex takes place in three consecutive steps, according to *Honma* and *Hagiwara* [17]. Initially the sulfite complex decomposes into gold(I) salt and sulfite ions. The gold(I) salt then hydrolyses and releases gold(I) ions (Au^+), which are subsequently reduced at the cathode to metallic gold:

$$[Au(SO_3)_2]^{3-} \leftrightarrow AuSO_3^- + SO_3^{2-} \quad <2>$$

$$AuSO_3^- \leftrightarrow Au^+ + SO_3^{2-} \quad <3>$$

$$Au^+ + e^- \rightarrow Au \quad <4>$$

According to the mechanism proposed above, the reduction peak observed during the cathodic scan at -0.5 V could be attributed to the reduction of gold(I) to metallic gold. The large oxidation peak observed at 0.7 V probably results from the oxidation of the sulfite (SO_3^{2-}) ions present in the solution to sulfate SO_4^{2-}. The small current plateau observed during the cathodic scan just prior to the reduction peak for gold(I) (0.0 V to -0.3 V) does not seem to be related to any electrochemical process, and may therefore result from an uncompensated resistance in the cell [18]. These results suggest that the electrodeposition of gold is feasible at potentials more cathodic than -0.5 V. Based on this finding, the electrodeposition of gold was subsequently investigated at -0.5 V and -0.7 V (vs. anode). These potential values

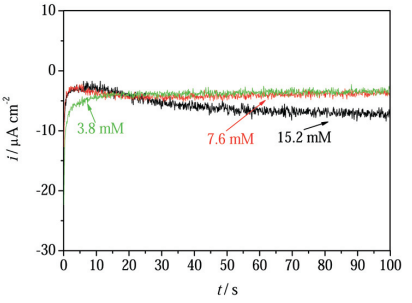

Fig. 5: Current transients obtained for the deposition of gold in the rhenium pores of a NiAl-Re eutectic in the presence of increasing concentrations of gold(I)

are approximated to the ones observed vs. SHE but taking into account the use of a two-electrode configuration. The electrodeposition of gold under potentials more positive than -0.5 V was negligible, and the process was more favoured when a potential of -0.7 V was applied. Therefore, further electrodeposition was done at this potential.

The current transients obtained for the electrodeposition of gold at -0.7 V from solutions with different concentrations of the gold(I) salt are shown in *Figure 5*. For a concentration of 15.2 mM gold(I) (black plot) the current density showed a sharp increase at short times, then reached a maximum at -2.3 μA/cm^2 (i_{max}) after only ~ 6.8 s (t_{max}), and decreased subsequently to a value of -7 μA/cm^2 (*Fig. 4*). A similar trend was observed when the deposition was carried out from a solution containing 7.6 mM of gold(I). In this case, the current reaches its maximum value of -2.41 μA/cm^2 (i_{max}) after ~5 s (t_{max}), and drops afterwards to -4 μA/cm^2 (light grey plot on *Figure 4*). This behaviour indicates that at the beginning of the process, radial diffusion dominates, and the deposits grow independently from each other. After long times (> 30 s), the diffusion zones overlap and the growth of the deposits is controlled by the linear diffusion towards the surface [19].

The current transient obtained for the electrodeposition of gold from a bath containing only 3.8 mM gold(I) showed a much smaller and less defined peak (grey plot on *Figure 5*), which spread over a longer period of time (up to 20 s, compared to 5 to 6 s in the previous cases). This can be explained by the lower concentration of gold(I) ions in the bulk solution, which would result in longer transport paths and thus a slower growth of the deposits. The smaller the concentration, the later the overlap of the diffusion zones takes place. As a result, the maximum appears at longer times, and the peak broadens. The fast growth observed for larger concentrations also results in a faster depletion of ions in the region around the growing nuclei, and thus their diffusion zones overlap. As a consequence, the peak is observed at much shorter times [19]. All three examples gave straight lines for plots of log(i) vs. log(t) with slope values of 0.5, in agreement with a process characterized by instantaneous nucleation [4, 20].

The most accepted model for the description of three dimensional nucleation followed by diffusion controlled growth establishes two cases: progressive and instantaneous nucleation, where the current and time are expressed respectively by the following equations [20, 21]:

for progressive nucleation

$$\left(\frac{i}{i_{max}}\right)^2 = 1.2254\left(\frac{t}{t_{max}}\right)^{-1}\left\{1-e^{-2.3367\left(\frac{t}{t_{max}}\right)^2}\right\}^2 \quad <5>$$

for instantaneous nucleation

$$\left(\frac{i}{i_{max}}\right)^2 = 1.9542\left(\frac{t}{t_{max}}\right)^{-1}\left\{1-e^{-1.2564\left(\frac{t}{t_{max}}\right)^2}\right\}^2 \quad <6>$$

where i_{max} and t_{max} are the maximum cathodic current and the time at which it was reached, respectively. The presence of one process or the other can be determined from the reduced plots depicting the current values as a function of the maximum current (i_{max}) against the time values as a function of the time at which this i_{max} is observed (t_{max}). The plots for i/i_{max} vs. t/t_{max} for each of the investigated cases are shown in *Figure 6*. Under the experimental conditions used, the electrodeposition of gold would be expected to follow an instantaneous nucleation, since the number of nuclei is limited to the density of rhenium fibres present on the structure, and therefore should reach a constant current value after

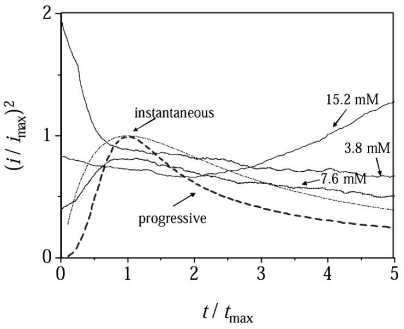

Fig. 6: Current-time transients' data plotted in reduced-variable form. The plots are compared to the theoretical ones expected for either an instantaneous or progressive nucleation process

all these fibres are host to gold deposits. However, a comparison of the plots given in *Figure 6* with those expected for either an instantaneous of progressive nucleation as described in the literature shows that this process does not follow any of the suggested models accurately for any of the solutions studied. Only for an electrolyte containing 7.6 mM gold(I) the plot resembled that of an instantaneous nucleation process.

For a more diluted concentration (3.8 mM), i/i_{max} reaches the diffusion controlled zone after the initial decay, and could then be better described by the *Cottrell equation*. This behavior would be expected for a more concentrated solution, but the fact that it is observed for the most diluted amount of gold(I) ions suggests that the deviation from ideal observed experimentally is due to other factors. A possible explanation could be the simultaneous occurrence of additional electrochemical processes, mainly reduction of the remaining rhenium fibres covered by oxides. The current due to this process would not be separated from the overall recorded current, and thus could yield to the misleading interpretation. For its effect to be negligible, the current due to the electrodeposition process must be dominant, as it seems to be the case for a solution containing 7.6 mM gold(I). For the case of 3.8 mM gold(I), the reduction of rhenium oxides may be the predominant process, resulting in a significant masking of the current due to an exclusive electrodeposition. However, some kinetic analyses could still be carried out from the data obtained for a gold(I) concentration of 7.6 mM. The number of deposits formed on the NiAl-Re sample after electrodeposition from this solution can be calculated according to [22–26]:

$$i_{max} = 0.6382\ z\ F\ D\ c\ (kN_0)^{1/2} \quad <7>$$

$$t_{max} = 1.5264/(N_0 \pi k D) \quad <8>$$

The calculated density of deposits corresponding to the electrodeposition of gold from a solution containing 7.6 mM gold(I) at -0.7 V is $6.4 \cdot 10^{13}$ cm^{-2}.

Figure 7 shows SEM images of the deposits obtained after electrodeposition for short time with diluted solutions of gold(I). It can be seen that the deposition for very short times from diluted concentrations of gold(I) yields gold deposits that cover almost exclusively the pores. For the most diluted concentrations studied (3.8 mM), even the deposition for long times (30 min.) does not produce large gold spheres. The method is therefore suitable for the initial aim of creating arrays of gold nanoelectrodes.

4 Conclusion

Kinetic analyses of the electrodeposition of gold on the nanopores formed in ds-NiAl-Re eutectic alloys were carried out as an essential step to understand the process and thus control the growth of the obtained structures. Image analyses of the gold deposits obtained when the electrodeposition process was done by application of short cathodic and anodic pulses showed an increase in the size of the deposited hemispheres with the duration of the cathodic pulse. The density of gold deposits increased after the application of the initial pulses, but remained fairly constant afterwards, when the nucleation step is overcome by the growth of the formed nuclei.

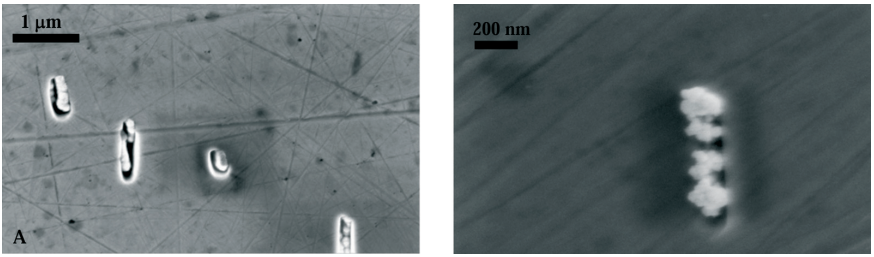

Fig. 7: Gold deposits obtained in rhenium pores by polarization of the samples at -0.7 V (vs. counter) from diluted solutions of the gold(I) salt: A) 15.2 mM gold(I), total deposition time 100 s; B) 3.8 mM gold(I), total deposition time 200 s

The formation of gold deposits seems to occur only after the application of a minimum charge (~ 800 C/m^2). The charge consumption is attributed to the simultaneous concurrence of other electrochemical processes, mainly reduction of rhenium oxides on the fibres, charging of the insulating oxide film on the NiAl matrix, and partial oxidation of the rhenium to perrhenate.

Analyses of the current transients were recorded when the electrodeposition was done under potentiostatic conditions and with diluted gold (Au(I)) solutions. The results were then used to determine the nucleation and growth processes taking place. It was observed that the current density increased at very short times due to a nucleation and three-dimensional growth of hemispherical islands.

At longer times, the diffusion fields for each nucleus start interacting and the current decreases. This decrease signals the transition to a one-dimensional limited growth, which can be described by the *Cottrell equation* (*eq. <7>*). The experimental data was not well correlated to theoretical models in all cases, possibly due to the effect of rhenium oxide reduction in the recorded current. However, the investigations remain useful to understand the electrochemistry behind the polarization and electrodeposition on complex metallic substrates. The gold hemispheres obtained when the deposition was done at short times and from diluted concentrations of the gold(I) ion grew almost exclusively into the pores, thus making this procedure suitable for the formation of arrays of gold nanoelectrodes.

Acknowledgements

The financial support of the Deutsche-Forschungs-Gemeinschaft through the project Application of Directionally Solidified Nanowire Arrays HA3118/4-3 & Functional Devices from Directionally Grown Nanowire Arrays HA3118/4-3 within the DFG Priority Program SPP1165 Nanowires and Nanotubes - from Controlled Synthesis to Function is gratefully acknowledged. The authors are also grateful to Dr. Srdjan Milenkovic for the solidification of the employed eutectics.

Contact

Achim Walter Hassel; e-mail: hassel@elchem.de

References

[1] Modern Electroplating: M. Schlesinger, M. Paunovic Eds., (2000), John Wiley & Sons

[2] Rosso, M.; Chassaing, E.; Fleury, V.; Chazalviel, J. N.; J. Electroanal. Chem. (2003) 559, 165-173.

[3] Serruya, A.; Mostany, J.; Scharifker, B. R.; J. Electroanal. Chem. (1999) 464 , 39–47

[4] Schultze, J. W.; Lohrengel, M. M.; Ross, D.; Electrochim. Acta (1983) 28, 973–984

[5] Stoychev, D.; Papoutsis, A.; Kelaidopoulou, A.; Kokkinidis, G.; Milchev. A.; Mat. Chem; Phys. (2001) 72, 360–365

[6] Depestel, L. M.; Strubbe, K.; J. Electroanal. Chem. (2004) 572, 195–201

[7] Dolati, A.; Ghorbani, M.; Ahmadi, M. R.; J. Electroanal. Chem. (2005) 577, 1–8

[8] Heerman, L.; Tarallo. A.; J. Electroanal. Chem. (1998) 451, 101–109

[9] Scharifker, B. R.; J. Electroanal. Chem. (1998) 458, 253–255

[10] Kolb, D. M.; Surface Science (2002) 500, 722–740

[11] Hassel, A. W.; Bello Rodriguez, B.; Milenkovic, S.; Schneider, A.; Electrochim. Acta (2005) 51, 795–801

[12] Milenkovic, S.; Hassel, A.W.; Schneider, A.; Nano Lett. (2006) 6, 794 –799

[13] Osaka, T.; Okinaka, Y.; Sasano, J.; Kato, M.; Sci. Techn. Advanc. Mater. (2006) 7, 425–437

[14] Dobrev, D.; Vetter, J.; Angert, N.; Neumann, R.; Electrochim. Acta (2000) 45, 3117–3125

[15] Bello Rodriguez, B.; Hassel, A. W.; J. Electrochem. Soc. (2006) 153, C33–C36

[16] Bello Rodriguez, B.; Hassel, A.W.; J. Electrochem. Soc. 155 (2008) K31–K37

[17] Honma, H.; Hagiwara, K.; J. Electrochem. Soc. (1995) 142, 81–87

[18] Radisic, A.; Vereecken, P. M.; Searson, P. C.; Ross. F. M.; Surf. Sci. (2006) 600, 1817–1826

[19] Nagy, G.; Denuault. G.; J. Electroanal. Chem. (1997) 433, 175–180

[20] Legrand, L.; Tranchant, A.; Messina, R.; J. Electrochem. Soc. (1994) 141, 378–382

[21] Scharifker, B.; Hills, G.; Electrochim. Acta (1983) 28, 879–889

[22] Scharifker, B. R.; Mostany, J.; J. Electroanal. Chem. (1984) 177, 13–23

[23] Kelber, J.; Rudenja, S., Bjelkevig, C.; Electrochim. Acta (2006) 51, 3086–3090

[24] Nagy, G.; Sugimoto, Y.; Denuault, G.; J. Electroanal. Chem. (1997) 433, 167–173

[25] Paunovic, M.; Schlesinger, M.: Fundamentals of Electrodeposition, Wiley Interscience (2006)

[26] Bard, A. J.; Faulkner, L. R.: Electrochemical Methods; Fundamentals and Applications; 2nd Ed. Wiley, New York (2001)

CONTACT:

EUGEN G. LEUZE VERLAG KG
Ralf Schattmaier
Karlstraße 4
88348 Bad Saulgau
Germany

Email: ralf.schattmaier@leuze-verlag.de
Phone: +49 0 7581 4801-12
Fax: +49 0 7581 4801-10